RESEARCH PAPER

Experimental Physiology WILEY

Angiotensin-II receptor type Ia does not contribute to cardiac atrophy following high-thoracic spinal cord injury in mice

Anne Järve[1,2] 🔴 | Fatimunnisa Qadri[1] | Mihail Todiras[1,3] 🔴 | Shirley Schmolke[1] |
Michael Bader[1,2,4,5]

[1] Max-Delbrück-Center for Molecular Medicine in the Helmholtz Association (MDC), Berlin, Germany

[2] DZHK (German Center for Cardiovascular Research), Partner Site Berlin, Berlin, Germany

[3] Nicolae Testemiţanu State University of Medicine and Pharmacy, Chisinau, Moldova

[4] Charité Universitätsmedizin Berlin, Berlin, Germany

[5] Institute for Biology, University of Lübeck, Lübeck, Germany

Correspondence
Anne Järve, Robert-Rössle-Str. 10, Berlin 13125, Germany
Email: anne.jaerve@mdc-berlin.de

Edited by: Carolyn Barrett

The copyright line for this article was changed on 30 December 2020 after original online publication.

[Correction added on 30 December 2020, after first online publlication: Projekt DEAL funding statement has been added.].

Funding information
Wings for Life, Grant/Award Number: 2014–2016; BIH Gender Equality Fund, Grant/Award Number: 2018

Abstract

Spinal cord injury (SCI) leads to cardiac atrophy often accompanied by functional deficits. The renin–angiotensin system (RAS) with angiotensin II (AngII) signalling via its receptor AT1a might contribute to cardiac atrophy post-SCI. We performed spinal cord transection at thoracic level T4 (T4-Tx) or sham-operation in female wild-type mice (WT, $n = 27$) and mice deficient in AT1a ($Agtr1a^{-/-}$, $n = 27$). Echocardiography (0, 7, 21 and 28 days post-SCI) and histology and gene expression analyses at 1 and 2 months post-SCI were performed. We found cardiac atrophy post-SCI: reduced heart weight, reduced estimated left ventricular mass in $Agtr1a^{-/-}$, and reduced cardiomyocyte diameter in WT mice. Although, the latter as well as stroke volume (SV) and cardiac output (CO) were reduced in $Agtr1a^{-/-}$ mice already at baseline, cardiomyocyte diameter was even smaller in injured $Agtr1a^{-/-}$ mice compared to injured WT mice. SV and CO were reduced in WT mice post-SCI. Ejection fraction and fractional shortening were preserved post-SCI in both genotypes. There were no histological signs of fibrosis and pathology in the cardiac sections of either genotype post-SCI. Gene expression of $Agtr1a$ showed a trend for up-regulation at 2 months post-SCI; $angiotensinogen$ was up-regulated at 2 month post-SCI in both genotypes. AngII receptor type 2 ($Agtr2$) was up- and down-regulated at 1 and 2 months post-SCI in WT mice, respectively, and Ang-(1-7) receptor (Mas) at 1 and 2 months post-SCI. $Atrogin-1/MAFbx$ and $MuRF1$, atrophy markers, were not significantly up-regulated post-SCI. Our data show that lack of AT1a does not protect from cardiac atrophy post-SCI.

KEYWORDS
atrogenes, cardiac atrophy, renin–angiotensin system

1 | INTRODUCTION

Cardiovascular dysfunction is a major problem for people with spinal cord injury (SCI), affecting both mortality and morbidity (Weaver, Fleming, Mathias, & Krassioukov, 2012). Development of cardiovascular risk factors (Cragg, Noonan, Krassioukov, & Borisoff, 2013) and potentially also cardiac pathology contribute to the elevated risk of heart disease in this patient group. Acute cardiac damage upon SCI in autopsy as well as in experimental animals is mediated by calcium excitotoxicity and massive noradrenaline release (Sharov & Galakhin, 1984). In chronic experimental SCI cardiac atrophy with systolic dysfunction and reduced contractility appear (Poormasjedi-Meibod et al., 2019; West et al., 2014), whereas in patients cardiac atrophy and stroke volume reduction are not accompanied by ejection

fraction reduction, and thus it is considered that no dysfunction exists (Driussi et al., 2014; Williams, Gee, Voss, & West, 2019). Cardiac atrophy results from loss of supraspinal sympathetic control over the heart and vasculature and cardiac unloading post-SCI, which is caused by reduced venous return and activity (Lujan & Dicarlo, 2014; Squair et al., 2018). Cardiac unloading in turn activates the ubiquitin-proteasome system (UPS) and the autophagy-lysosomal machinery (Poormasjedi-Meibod et al., 2019; Zaglia et al., 2013). Further research is required in order to identify and verify players in this physiological or pathological process.

The renin–angiotensin system (RAS) and activation of its classical axis with elevated angiotensin II (AngII) and expression of one of its G-protein-coupled receptors, AngII receptor type 1a (AT1a), could be a double-edged sword in the heart following SCI (Groothuis et al., 2010; Mathias, Christensen, Frankel, & Peart, 1980; Poormasjedi-Meibod et al., 2019). For example, AngII/AT1a signalling aggravates skeletal muscle atrophy by activation of UPS and autophagy (Burks et al., 2011; Cabello-Verrugio, Cordova, & Salas, 2012). Furthermore, blocking of this signalling has prevented left ventricular remodelling in a cachexic cardiac model (Stevens et al., 2015; Yoshida et al., 2013). At the same time, AngII/AT1a is mediating myocyte hypertrophy, fibroblast proliferation, collagen synthesis, smooth muscle cell growth, endothelial adhesion molecule expression and catecholamine synthesis (Regitz-Zagrosek, Fielitz, & Fleck, 1998). The role of AngII/AT1a following SCI remains unclear.

We hypothesized that mice lacking AT1a would present less cardiac atrophy and dysfunction post-SCI, e.g. by less activated UPS. If so, this could provide a therapeutic strategy to protect the heart post-SCI. To test this hypothesis, we performed spinal cord transection at thoracic level T4 (T4-Tx), which is supposed to lead to reduction of approximately 75% of sympathetic innervation to the heart from the stellate ganglion (Strack, Sawyer, Marubio, & Loewy, 1988), or sham-operation in WT and $Agtr1a^{-/-}$ mice. We investigated heart structure/function by echocardiography combined by histological and gene expression analysis at 1 and 2 months post-SCI.

2 | MATERIALS AND METHODS

2.1 | Ethical approval

Experiments were conducted according to the National Institutes of Health *Guide for the Care and Use of Laboratory Animals*, and the ethical principles under which the journal operates: our work complies with the journal's animal ethics checklist. The protocols were approved by the local Animal Care and Use Committee from Berlin LAGeSo (G0132/14).

2.2 | Mice and experimental protocol

All mice were housed in groups of four to six animals in cages with nesting material, mouse lodges and open access to water and food, at

New Findings

- **What is the central question of this study?**
  What is the role of the renin–angiotensin system with angiotensin II acting via its receptor AT1a in spinal cord injury-induced cardiac atrophy?

- **What is the main finding and its importance?**
  Knockout of AT1a did not protect mice that had undergone thoracic level 4 transection from cardiac atrophy. There were no histopathological signs but there was reduced load-dependent left ventricular function (lower stroke volume and cardiac output) with preserved ejection fraction.

23°C with a 12 h/12 h circadian cycle. Experiments were performed using female wild-type C57Bl/6 J (WT, $Agtr1a^{+/+}$) *vs.* AT1a receptor-deficient mice (B6.129P2-$Agtr1a^{tm1Unc}$/J from The Jackson Laboratory, Bar Harbor, MA, USA) ($Agtr1a^{-/-}$), weighing 20–25 g, and at about 3 months of age.

The first group of mice ($Agtr1a^{+/+}$ sham $n = 6$, SCI $n = 7$; $Agtr1a^{-/-}$ sham $n = 5$, SCI $n = 8$) were killed with an overdose of intraperitoneal ketamine (140 mg kg^{-1})–xylazine (14 mg kg^{-1}) anaesthesia 1 month post-SCI. The second group ($Agtr1a^{+/+}$ sham $n = 7$, SCI $n = 7$; $Agtr1a^{-/-}$ sham $n = 7$, SCI $n = 7$) was killed as described above at 2 months post-SCI. Cardiac tissue from both 1- and 2-month groups was analysed by histology and qPCR. All data analysis (echocardiography, histology, qPCR, cardiomyocyte diameter) was conducted with the experimenter blinded to the different genotype and injury/sham group, except in the echocardiography injury/sham group, where the experimenter could not be blinded.

2.3 | SCI

SCI was performed under intraperitoneal ketamine (100 mg kg^{-1})–xylazine (10 mg kg^{-1}) anaesthesia in combination with isoflurane (1.5–1.8%) inhalation as described previously (Jarve et al., 2018). Briefly, a dorsal midline incision was made in the superficial muscle overlying the C7–T3 vertebrae. The dura was opened at the T2–T3 intervertebral gap and the spinal cord was completely transected using microscissors. Complete transection was confirmed by pulling a needle twice between the rostral and caudal spinal cord stumps. Gelfoam was placed above spinal cord to achieve haemostasis. The muscle and skin were closed with absorbable sutures (Vicryl, 4–0, Ethicon GmbH, Norderstedt, Germany). Animals received warmed saline (1 ml, s.c.), recovered and were kept in heated cages (30°C) for the rest of the experiments. For analgesia mice were treated with carprofen (4 mg kg^{-1}, s.c.) directly after operation and the next day with a 12 h interval, if necessary longer. The bladder was manually emptied three times daily for the whole duration of the experiment.

2.4 | Echocardiographic studies

Two-dimensional echocardiographic imaging was performed under isoflurane anaesthesia 1 day before and 7, 21 and 28 days post-injury/sham-surgery (dpi) using the Vevo 700 high-resolution in vivo ultrasound technology (VisualSonics, Toronto, Canada) equipped with an MS-400 scan head with transmission frequency of 30 MHz. Anaesthesia was induced with isoflurane 3% and maintained with (1.6 vol% isoflurane–air). Body temperature was maintained through a heating pad at 37°C. Images were acquired for further off-line analysis by a single operator of the Max Delbrück Center for Molecular Medicine Animal Phenotyping Platform blinded for genotype. Left ventricular (LV) end-diastolic and end-systolic diameter (LVIDd, LVIDs), ejection fraction (EF), stroke volume (SV) and heart rate (HR) were determined by tracing of endocardial and epicardial borders and majors in end-diastole and in end-systole in the parasternal long axis view. LV end-diastolic and end-systolic posterior wall thickness (PWTd, PWTs) and anterior wall (interventricular septal wall) thickness (IVSd, IVSs) were determined by tracing at end-diastole and at end-systole in the parasternal short axis view. Fractional shortening (FS, %), cardiac output (CO, ml min^{-1}) and LV mass were calculated:

$$FS = 100 \times [(LVIDd – LVIDs)/LVIDd]$$
$$CO = SV \times HR/1000$$
$$LV\ mass = 1.053 \times [(LVIDd + LVPWd + IVSd)^3 – LVIDd^3].$$

2.5 | Quantitative RT-PCR

Hearts were halved so that the apex-facing part was processed further for RNA isolation and real-time qPCR analysis and the upper part was used for histology. For RNA isolation with Trizol and FastPrep beads, the manufacturer's instructions were followed. Reverse transcription was performed with 2 μg total RNA using Moloney murine leukaemia virus with digestion by incubation with 1 μl DNase I (Roche Applied Science, Mannheim, Germany). Real-time PCR was performed with a QuantStudio 5 Real-Time PCR System (Thermo Fisher Scientific, Waltham, MA, USA) according to the manufacturer's recommendations by using SYBR Green; the amplicon detected by SYBR Green was verified by a melting point analysis. Each cDNA sample was tested in triplicate, and the expression level of each gene was normalized to the hypoxanthine-guanine phosphoribosyltransferase (Hprt) level. The primers used are listed in Table 1. The fold change was determined using the $2^{-\Delta\Delta C_t}$ method.

2.6 | Histology

Hearts were dissected without the great vessels and their weight determined. Upper halves of the hearts were incubated in KCl for 10 min, fixed for 48 h in 4% paraformaldehyde in buffered saline (pH 7.4) at 4°C, washed, dehydrated, embedded in paraffin, sectioned at 5 μm with a rotary microtome (Microm; Thermo Fisher Scientific),

TABLE 1 Quantitative real-time PCR targets and their primer sequences

| Primer	Forward and reverse sequence 5′-3′
Ubiquitin proteasome pathway	
Murf1	Forward: 5′-TGACATCTACAAGCAGGAGTGC-3′ Reverse: 5′-TCGTCTTCGTGTTCCTTGC-3′,
MAFbx	Forward: 5′-AGTGAGGACCGGCTACTGTG-3′ Reverse: 5′-GATCAAACGCTTGCGAATCT-3′
Renin–angiotensin system	
Agtr1a	Forward: 5′-CCATTGTCCACCCGATGAAG-3′ Reverse: 5′-TGCAGGTGACTTTGGCCAC-3′,
Agtr2	Forward: 5′-CAATCTGGCTGTGGCTGACTT-3′ Reverse: 5′-TGCACATCACAGGTCCAA AGA-3′
angiotensinogen	Forward: 5′-TGTGACAGGGTGGAAGATGA-3′ Reverse: 5′-CAGGCA GCTGAGAGAAACCT-3′
Mas	Forward: 5′-AGGGTGACTGACTGAGTTTGG-3′ Reverse: 5′-GAAGGTAAGAGGACAGGAGC-3′
Housekeeping	
Hprt	Forward: 5′-GTAATGATCAGTCAACGGGGG AC-3′ Reverse: 5′-CCAGCAAGCTTGCAACCTTAACCA- 3′

Murf1, muscle ring finger 1; *MAFbx*, muscle atrophy F-box; *Agt*, angiotensinogen; *Agtr1a*, Ang II type 1 receptor type a; *Agtr2*, Ang II type 2 receptor; *Mas*, MAS1 proto-oncogene, G protein-coupled receptor.

placed on SuperFrost Plus slides (Thermo Fisher Scientific) and stored at room temperature until use. For picro-Sirius red staining, paraffin sections were deparaffinized, rehydrated and stained by incubation with picro-Sirius red solution (0.1% Sirius red F3B in saturated aqueous solution of picric acid) for 1 h at room temperature. After two washes with acidified water (0.5% glacial acetic acid in tap water), sections were dehydrated in three changes of 100% ethanol, cleared using xylene and coverslipped using Eukitt (ORSAtec GmbH, Bobingen, Germany). Four non-consecutive sections with haematoxylin–eosin (HE) and Sirius red staining per mouse were analysed using an inverted microscope (BZ-9000; Keyence, Osaka, Japan).

For quantification of cardiomyocyte diameter, at the mid-ventricular level wheat germ agglutinin (WGA) staining was performed by incubating deparaffinized and rehydrated heart sections with WGA+Al488 conjugate (1:300) (Thermo Fisher Scientific) for 20 h at 4°C, washed three times with phosphate-buffered saline for 10 min each and coverslipped using Vectashield (Vecta Laboratories, Burlingame, CA, USA) mounting medium containing 4′,6-diamidino-2-phenylindole. To evaluate cardiomyocyte diameter, images were taken using an inverted microscope (BZ-9000) and 610–980 cardiomyocytes per group were analysed using BZ-II Analyzer software (Keyence).

2.7 | Power analysis

There has been no previous echocardiography study in mice with SCI. A power analysis based on the study of West et al. (2014) in rats with SCI showed that a sample size of two mice per group has a 80% power to detect a 12% change of LVIDd, 26% change of SV and 28% change in

Legend:
- ● WT sham (n=6)
- ■ WT T4-Tx (n=7)
- ▲ Agtr1a⁻/⁻ sham (n=5)
- ▼ Agtr1a⁻/⁻ T4-Tx (n=8)
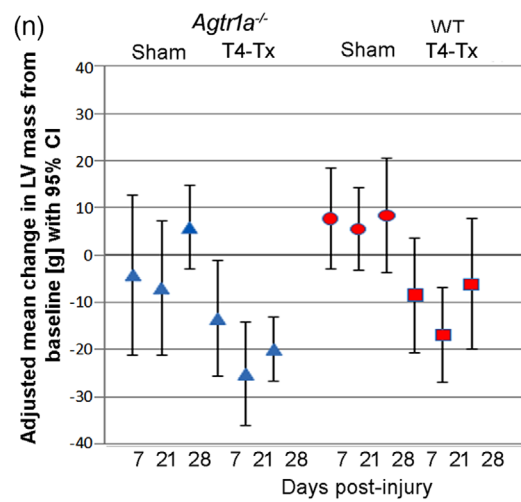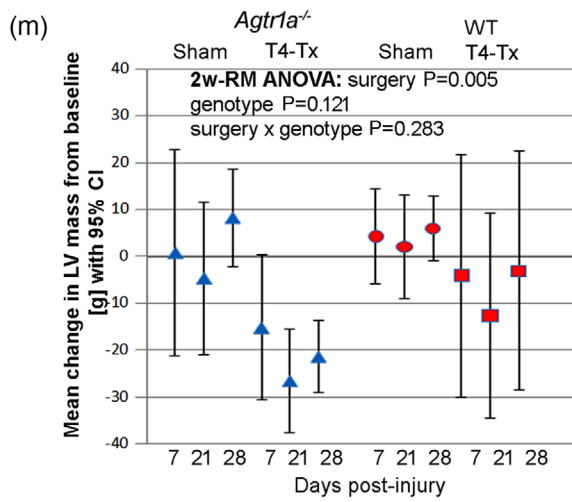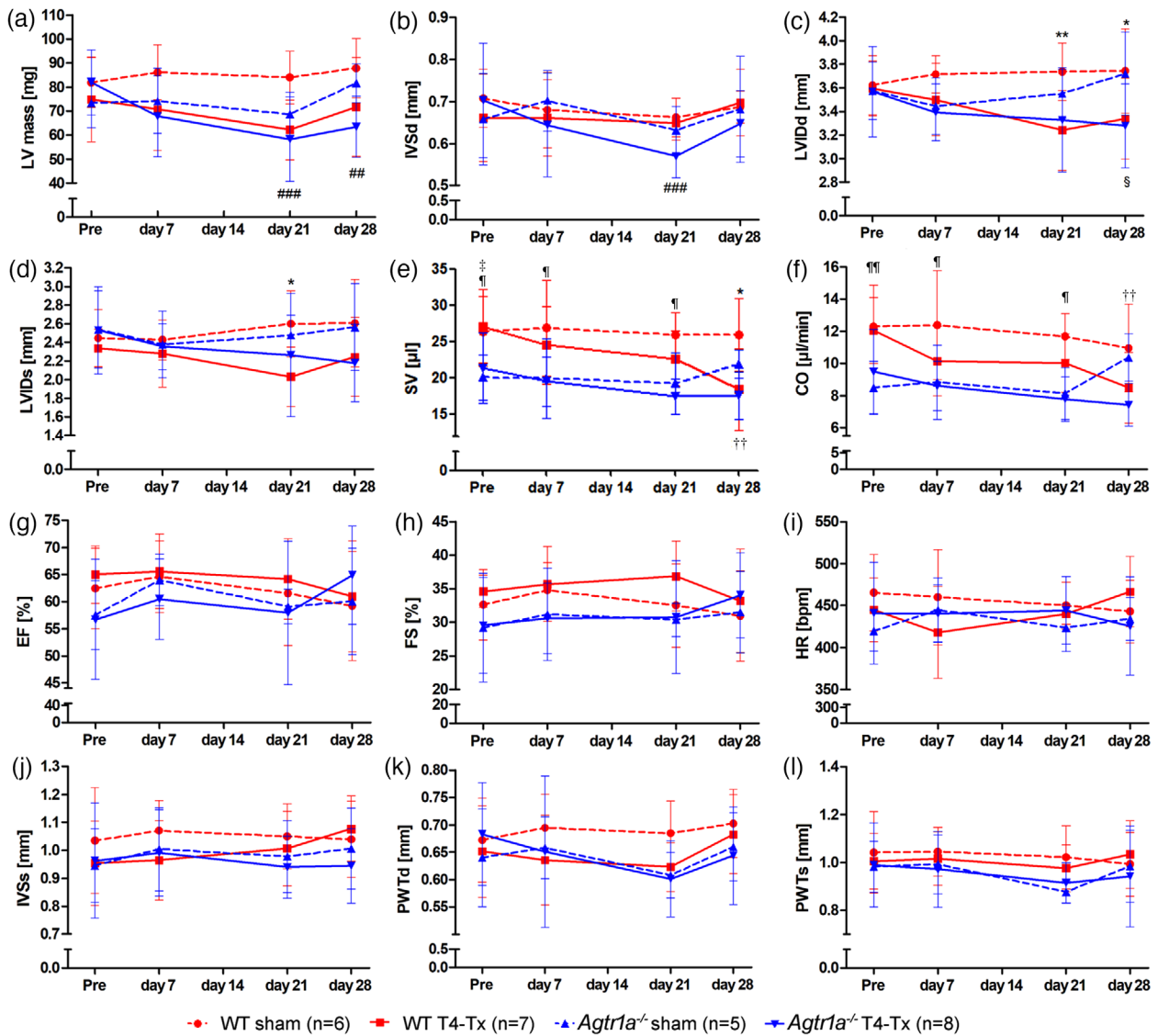
CO, assuming a 5% significance level and a two-sided test. Our previous echocardiography study of mice 1 month post-myocardial infarction showed that we would need seven to eight mice in order to see a 12% change of LVIDd and 25% change in FS assuming a 5% significance level and a two-sided test. Therefore, the group size in echocardiography experiment was five to eight mice.

2.8 | Statistics

Data were analysed statistically using Prism 5 software (GraphPad Software, San Diego, CA, USA) and SPSS Statistics (IMB Corp., Armonk, NY, USA). Echocardiography data were analysed using two-way repeated measures (RM) ANOVA with a Bonferroni *post hoc* test. Two-way ANOVA was conducted on the influence of two independent factors (surgery and genotype) on heart weight and cardiomyocyte diameter. Surgery type included two levels (sham and SCI) and genotype consisted of two levels (WT, KO). qPCR data fold changes were analysed with one-way ANOVA followed by a *post hoc* test. Significance for all tests was assumed when $P < 0.05$. Results are presented as means $\pm$ SD.

3 | RESULTS

3.1 | Echocardiography: reduced SV and CO, but preserved FS and EF post-SCI

Structural changes following SCI observed in echocardiography included reduction of the estimated LV mass at 21 and 28 dpi (2-way RM ANOVA Bonferroni *post hoc* test, $P < 0.001$ and $P < 0.01$) as well as of IVSd at 21 dpi in $Agtr1a^{-/-}$ mice *vs.* pre-injury values in these mice (2-way RM ANOVA Bonferroni *post hoc* test, $P < 0.001$) (Figure 1a,b). LVIDd was smaller in injured *vs.* sham WT mice at 21 and 28 dpi (2-way RM ANOVA Bonferroni *post hoc* test, $P < 0.01$ and $P < 0.05$) as well as in injured *vs.* sham $Agtr1a^{-/-}$ mice at 28 dpi (2-way RM ANOVA Bonferroni *post hoc* test, $P < 0.05$) (Figure 1c). LVIDs was smaller in WT sham *vs.* injured mice at 21 dpi (2-way RM ANOVA Bonferroni *post hoc* test, $P < 0.05$) (Figure 1d). Functional changes upon SCI comprised a reduced SV at 28 dpi in WT sham *vs.* WT injured mice and within WT injured mice *vs.* pre-injury values (2-way RM ANOVA Bonferroni *post hoc* test, $P < 0.05$ and $P < 0.01$) (Figure 1e). SV was lower in $Agtr1a^{-/-}$ sham mice *vs.* WT sham mice (pre-surgery, 7, 21 days post-surgery) and in baseline measurement of T4-Tx WT

vs. T4-Tx $Agtr1a^{-/-}$ mice (2-way RM ANOVA Bonferroni *post hoc* test, all $P < 0.05$). CO was lower following SCI in WT mice at 28 dpi *vs.* pre-injury (2-way RM ANOVA Bonferroni *post hoc* test, $P < 0.01$) and in $Agtr1a^{-/-}$ sham *vs.* WT sham (pre-surgery, 7, 21 days post-surgery 2-way RM ANOVA Bonferroni *post hoc* test, all $P < 0.05$) (Figure 1f). There were no significant differences in EF and FS post-SCI, nor in HR, IVSs, LVIDs, PWTd and PWTs (2-way RM ANOVA Bonferroni *post hoc* test, all $P > 0.05$) (Figure 1g–l). Two-way RM ANOVA did not reveal any significant interaction between the treatment group and the time factor for any of the analysed echocardiography parameters. For LV mass the interaction effect has borderline significance ($P = 0.0551$). In order to investigate whether the effect of SCI on LV mass is different in $Agtr1a^{-/-}$ mice compared to WT, we plotted the mean difference in the change in LV mass with SCI *vs.* sham in WT *vs.* knockout mice, together with 95% confidence intervals (CI), at each time point post-surgery (Figure 1m) and the adjusted mean differences (Figure 1n). LV mass decreased at 7 dpi (−15.2 (95% CI: 0.3, −30.7) g), at 21 dpi (−26.6 (95% CI: −16.3, −36.9) g) and at 28 dpi (−21.4 (95% CI: −13.7, −29.1) g) in KO, and at 7 dpi (−4.1 (95% CI: 21.8, −30.0) g), at 21 dpi (−12.6 (95% CI: 9.3, −34.5) g) and at 28 dpi (−3.1 (95% CI: 22.4, −28.6) g) in WT.

3.2 | Reduced cardiac weight and cardiomyocyte diameter following SCI, but proportional to body weight reduction

Mice with SCI had smaller heart weight (HW) and HW/tibia length ratios (HW/TBL) compared to sham mice independent of their genotype at 1 and 2 months post-SCI (2-way ANOVA, all $P < 0.006$) (Figure 2a,b). There was no statistically significant interaction between the effects of surgery and genotype level in HW or HW/TBL at 1 and 2 months post-SCI (all $F < 0.949$, $P > 0.340$. Main effect of genotype was also not significant (all $F < 1.807$, $P > 0.196$).

The ratio of HW/body weight (BW) did not differ between sham and injured mice of both genotypes, but tended to be smaller in the sham $Agtr1a^{-/-}$ mice compared to WT sham mice (2-way ANOVA, both $P > 0.090$) (Figure 2c).

Histological analysis of the diameter of cardiomyocytes at the mid-ventricular level was performed. Two-way ANOVA revealed a significant interaction between surgery type (T4-Tx *vs.* sham) and genotype (WT *vs.* KO) ($P < 0.0001$). The main effects of surgery and genotype both reached the higher significance ($P < 0.0001$) (Figure 2d).

FIGURE 1 Echocardiography before and after SCI in the WT and $Agtr1a^{-/-}$ mice. (a) Left ventricular mass (LV), (b) interventricular septum thickness at diastole (IVSDd), (c) LV internal diameter at diastole (LVIDd), (d) LV internal diameter at systole (LVIDs), (e) stroke volume (SV), (f) cardiac output (CO). (g–l) Ejection fraction (g) and fractional shortening (FS) (h), heart rate (HR) (i) and interventricular septum thickness at systole (IVSs) (j), and posterior wall thickness at diastole (PWTd) (k) and systole (PWTs) (l) were not regulated post-SCI. Two-way RM ANOVA with Bonferroni *post hoc* test: ##$P < 0.01$, ###$P < 0.001$, KO pre- *vs.* post-SCI; *$P < 0.05$, **$P < 0.01$, WT sham *vs.* WT SCI; †$P < 0.05$, ††$P < 0.01$, WT pre *vs.* post-SCI; ‡$P < 0.05$ WT SCI *vs.* KO SCI; §$P < 0.05$ KO sham *vs.* KO SCI; ¶$P < 0.05$, ¶¶$P < 0.01$, WT sham *vs.* KO sham. Data are displayed as means $\pm$ SD. (m) Mean change in LV mass (LV mass at given time point is subtracted from pre-surgery value) and 95% confidence interval at indicated time points in $Agtr1a^{-/-}$ sham and SCI mice and $Agtr1a^{+/+}$ sham and SCI mice, (n) the same analyses adjusted for chance imbalance at baseline by including baseline LV mass as covariate
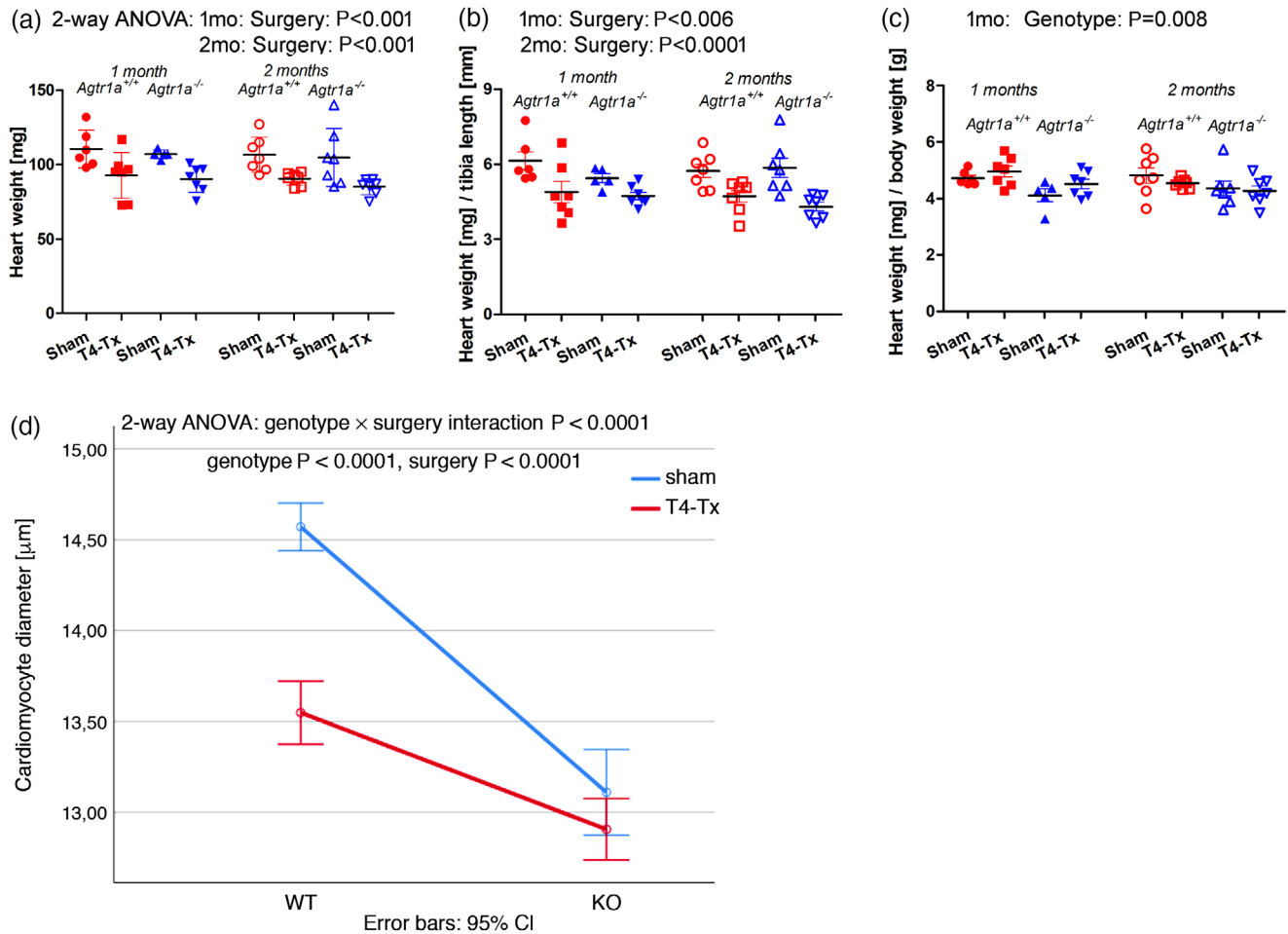
FIGURE 2 Cardiac atrophy and cardiomyocyte diameter post-SCI. (a–c) Heart weight (a) and its ratio with tibia length (b), but not its ratio with body weight (c) were reduced in injured *vs.* sham mice at 1 and 2 months post-SCI. (d) Cardiomyocyte diameter mean values with 0.95% confidence intervals 1 month post-surgery. Significant results of 2-way ANOVA are presented above the figures. WT sham 1 month $n = 6$ and 2 months $n = 7$; WT T4-Tx 1 month $n = 7$ and 2 months $n = 7$, $Agtr1a^{-/-}$ sham 1 month $n = 5$ and 2 months $n = 7$; $Agtr1a^{-/-}$ T4-Tx 1 month $n = 8$ and 2 months $n = 7$

3.3 | No signs of inflammation or fibrosis 1 month post-SCI

The myocardium of SCI mice had normal histology, with no signs of infiltration of monocytes and macrophages, cardiomyocyte necrosis in HE stained cardiac slices. Picro-Sirius red staining revealed no significant blood vessel-associated or interstitial fibrosis (Figure 3).

## 3.4 | Atrogene and RAS expression post-SCI

Next we investigated the regulation of the genes involved in atrophy and members of the RAS. Gene expression of muscle atrophy F-box (*MAFbx*) showed a trend for down-regulation and up-regulation at 1 and 2 month post-SCI, respectively, in WT mice compared to sham (1-way ANOVA, $P > 0.05$) and RING-finger protein-1 (*Murf1*) had no significant regulation (1-way ANOVA, $P > 0.05$) (Figure 4a,b). *Angiotensinogen* was up-regulated at 2 months post-SCI in $Agtr1a^{-/-}$

and WT mice compared to sham (1-way ANOVA with Bonferroni *post hoc* test, all $P < 0.05$) (Figure 4c). AngII receptor AT2 (*Agtr2*) was up-regulated at 1 month post-SCI in WT mice (1-way ANOVA with Bonferroni *post hoc* test, $P < 0.05$) (Figure 4d). The expression of *Mas* was down-regulated at 1 and 2 months post-SCI in WT and at 2 months post-SCI in knockout mice (1-way ANOVA with Bonferroni *post hoc* test, all $P < 0.05$) (Figure 4e). *Agtr1a* was not significantly regulated (1-way ANOVA with Bonferroni *post hoc* test, both $P > 0.05$) (Figure 4f).

4 | DISCUSSION

Major findings of this study include: (i) cardiac atrophy post-SCI with reduced HW at 1 and 2 months post-SCI in WT and $Agtr1a^{-/-}$ mice compared to sham mice; reduced cardiomyocyte diameter at 1 month post-SCI in WT mice; (ii) reduced SV and CO in WT mice at 1 month post-SCI; (iii) preserved EF and FS at 1 month post-SCI in WT and $Agtr1a^{-/-}$ mice; (iv) no cardiac pathology and fibrosis at 1 and 2 months

FIGURE 3 Cardiac histology post-SCI was unchanged compared to sham mice. Representative images of hematoxylin staining (a–f) and Sirius red staining (g–l). Scale bar: 500 μm
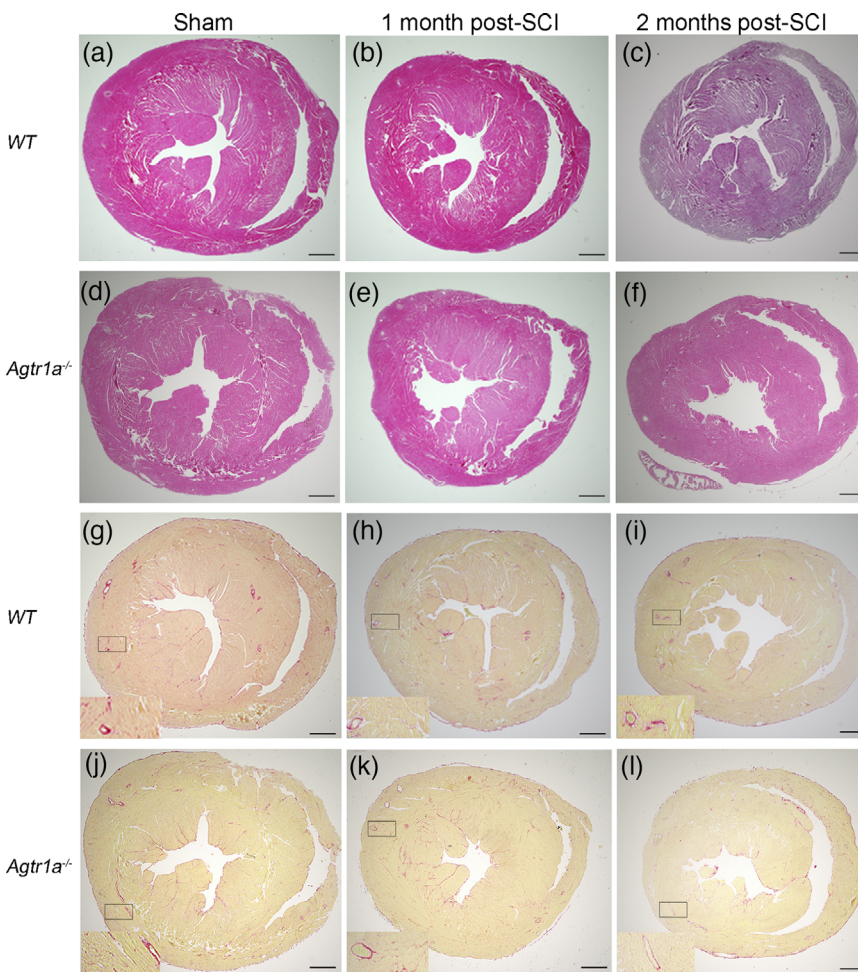
post-SCI; and (v) smaller cardiomyocyte diameter, SV and CO in non-injured $Agtr1a^{-/-}$ mice compared to WT mice.

Cardiac atrophy post-SCI is caused by loss of sympathetic innervation (trophic support) to the heart as well as by haemodynamic unloading, which is a result of reduced blood volume and physical inactivity (Lujan & Dicarlo, 2014; Squair et al., 2018; West et al., 2014). In our T4-Tx model, approximately 75% of sympathetic innervation to the heart from the stellate ganglion must be lost (Strack et al., 1988) resulting in approximately 18% lighter hearts in injured mice. In comparison, total chemical denervation leads to about 15% reduction in HW and this could be prevented by β_2-adrenoceptor stimulation, confirming the trophic effect of sympathetic input (Zaglia et al., 2013). Bed rest for 6 weeks, on the other hand, resulted in 8% reduced LV mass (Perhonen et al., 2001). Cardiac atrophy post-SCI likely reflects physiological adaption to the changed situation, rather than being pathological. Lack of dramatic histological changes or fibrosis and preserved EF and FS also support the idea of physiological remodelling. Activation of the UPS and autophagy mediates cardiac atrophy following denervation. In the SCI, UPS activation occurs at the same time as atrophy in the Zucker rat (Poormasjedi-Meibod et al., 2019). In our study, UPS was not changed at 2 months post-SCI, and it might need more time to be up-regulated or it may also be that these systems have been up-regulated early after SCI and later down-regulated when

physiological remodelling was completed. The species difference could be also responsible for this discrepancy between mice and rats.

Could cardiac atrophy be mediated by AngII/AT1a similar to skeletal muscle atrophy? Prerequisites for that are fulfilled. AngII levels and expression of $Agtr1a$ at 3 months post-SCI have been reported to be elevated (Groothuis et al., 2010; Poormasjedi-Meibod et al., 2019). In agreement with this, we observed a trend for up-regulation of $Agtr1a$ at 2 months post-SCI. Our hypothesis that AT1a contributes to the cardiac atrophy post-SCI was not confirmed, because $Agtr1a^{-/-}$ mice hearts were not less atrophied post-SCI. Indeed, the opposite might be true. LV mass and IVSd were significantly reduced following SCI, and cardiomyocyte diameter at 1 month post-SCI was smaller in the knockout mice indicating that AT1a contributes to trophic support to the heart after SCI. Without SCI, HW/BW of $Agtr1a^{-/-}$ mice tended to be smaller similarly to a previous report (Gembardt et al., 2008). Cardiomyocyte diameter was also smaller compared to sham WT mice. Thus, physiological signs of atrophy in $Agtr1a^{-/-}$ mice before and progression of atrophy following SCI indicates the importance of AT1a for cardiomyocyte growth stimulation in the heart (also not compensated by $Agtr1b$, the expression level of which is very low in the heart). Note that, except for smaller size, hearts of $Agtr1a^{-/-}$ mice are structurally normal and there is no dysfunction in echocardiography as we and others found (Gembardt et al., 2008; Sato et al., 2013).
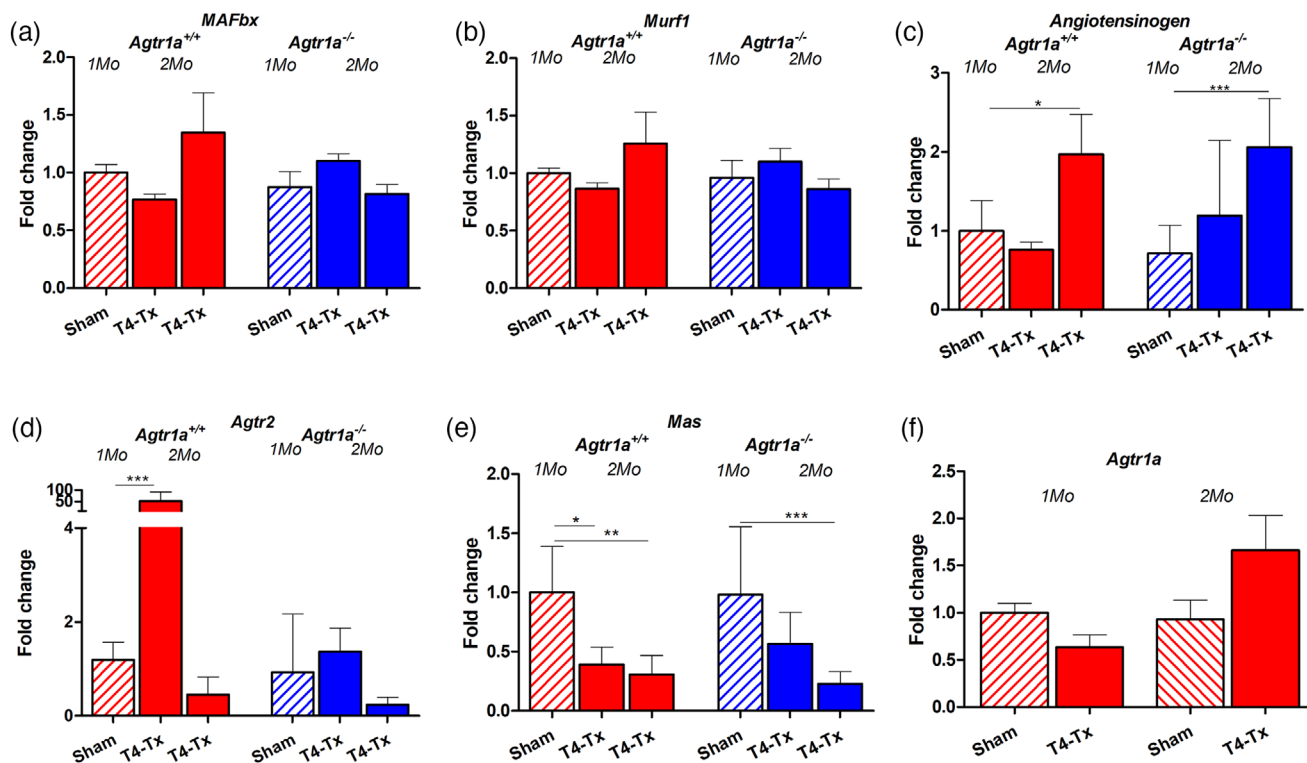
FIGURE 4 Gene expression of atrogenes and RAS members in the heart at 1 month and 2 months post-SCI in WT and *Agtr1a*$^{-/-}$ mice. (a) No regulation in muscle atrophy F-box (*MAFbx*) and (b) muscle ring finger 1 (*Murf1*) expression. (c) Up-regulation of *angiotensinogen* at 2 months post-SCI. (d) Up-regulation of *Agtr2* in WT mice at 1 month post-SCI. (e) *Mas* was down-regulated at 1 and 2 months post-SCI in WT and at 2 months in *Agtr1a*$^{-/-}$ mice. (f) *Agtr1a* was not significantly regulated. *$P < 0.05$, **$P < 0.01$, ***$P < 0.001$, 1-way ANOVA with Bonferroni *post hoc* test. WT sham $n = 10$; WT T4-Tx 1 month $n = 7$ and 2 months $n = 7$; *Agtr1a*$^{-/-}$ sham $n = 9$; *Agtr1a*$^{-/-}$ T4-Tx 1 month $n = 8$ and 2 months $n = 7$

Would blocking of the AngII/AT1 pathway be beneficial to the heart post-SCI similar to the cardiac cachexia model? Blocking of AngII/AT1a pathway by losartan in a model of murine tumour-induced cachexia prevented both the LV wall thinning and the decrease in EF and lowered cardiac gene expression levels of MAFbx and autophagy genes (Stevens et al., 2015). On the other hand improved function and remodelling noted in the tumour-bearing mice treated with losartan could also be caused by a significant hypotensive effect of losartan, e.g. by decrease in afterload (Scherrer-Crosbie, 2015). Because of prevalent hypotension post-SCI (Jarve et al., 2018), blocking of the AngII/AT1a axis would be detrimental following SCI. No beneficial effect to the heart could be expected, which is the opposite of the situation of hypertension and overload where blocking of AngII/AT1 activation protects from hypertrophy and fibrosis of the heart (Kurdi & Booz, 2011).

We observed no fibrosis in the heart post-SCI in contrast to an earlier report on a trend for higher signal for collagen I in cardiac sections post-SCI (West et al., 2014). In the human heart, AngII does not directly increase collagen or fibronectin mRNA (Kupfahl et al., 2000). AT1 is not (or its absence is not) connected to the basal production of connective tissue in the heart (van Esch et al., 2010). Thus, in the absence of obvious inflammation in the heart as after SCI in contrast to myocardial infarction, activation of the RAS is not contributing to fibrosis.

4.1 | Limitations

With small group sizes this study does not have sufficient power and precision to statistically undermine all detected effects, and therefore some findings must be confirmed in the future with a larger number of animals. EF was used here as the only measure of cardiac function. This might be critical in the setting of SCI, in which extreme changes in volume occur (Poormasjedi-Meibod et al., 2019; Williams et al., 2019). In further studies also parameters related to diastolic function (E, A, E/A) should be measured. As mice with SCI did not recover bladder function during the experiments, we cannot exclude the possibility that manual emptying of bladders might have affected our results, e.g. by inducing autonomic dysreflexia. However, we consider the possible effect negligible, taking into account that an hour-long similar procedure for a month would cause further reduction of basal contractility but not any significant structural alterations in the heart of exposed animals above that which is observed with SCI alone (West et al., 2016). Because we used only female mice, to draw a conclusion for the entire population further experiments including male mice are warranted. Since a global knockout was used, the possibility exists that physiological responses to the knockout in tissues other than the heart might in some unforeseen way compensate.

5 | CONCLUSION

The present study showed that absence of AT1a does not prevent cardiac atrophy post-SCI. Instead, AngII/AT1a seems to exert trophic support to the heart before and after SCI.

COMPETING INTERESTS
None.

AUTHOR CONTRIBUTIONS
A.J., F.Q., M.T. and S.S. performed the experiments. A.J. and S.S. analysed the data. A.J. and M.B. designed the research and wrote the manuscript. All authors approved the final version of the manuscript and agree to be accountable for all aspects of the work in ensuring that questions related to the accuracy or integrity of any part of the work are appropriately investigated and resolved. All persons designated as authors qualify for authorship, and all those who qualify for authorship are listed.

DATA AVAILABILITY STATEMENT
The data that support the findings of this study are available on request from the corresponding author. The data are not publicly available due to privacy or ethical restrictions.

ORCID
Anne Järve https://orcid.org/0000-0003-2096-0706
Mihail Todiras https://orcid.org/0000-0002-9373-4753

REFERENCES

Burks, T. N., Andres-Mateos, E., Marx, R., Mejias, R., Van Erp, C., Simmers, J. L., … Cohn, R. D. (2011). Losartan restores skeletal muscle remodeling and protects against disuse atrophy in sarcopenia. *Science Translational Medicine*, 3, 82ra37.

Cabello-Verrugio, C., Cordova, G., & Salas, J. D. (2012). Angiotensin II: Role in skeletal muscle atrophy. *Current Protein & Peptide Science*, 13, 560–569.

Cragg, J. J., Noonan, V. K., Krassioukov, A., & Borisoff, J. (2013). Cardiovascular disease and spinal cord injury: Results from a national population health survey. *Neurology*, 81, 723–728.

Driussi, C., Ius, A., Bizzarini, E., Antonini-Canterin, F., d'Andrea, A., Bossone, E., & Vriz, O. (2014). Structural and functional left ventricular impairment in subjects with chronic spinal cord injury and no overt cardiovascular disease. *Journal of Spinal Cord Medicine*, 37, 85–92.

Gembardt, F., Heringer-Walther, S., Esch, J. H. M.v, Sterner-Kock, A., Veghel, R. V., Le, T. H., … Walther, T. (2008). Cardiovascular phenotype of mice lacking all three subtypes of angiotensin II receptors. *FASEB Journal*, 22, 3068–3077.

Groothuis, J. T., Thijssen, D. H., Rongen, G. A., Deinum, J., Danser, A. H., Geurts, A. C., … Hopman, M. T. (2010). Angiotensin II contributes to the increased baseline leg vascular resistance in spinal cord-injured individuals. *Journal of Hypertension*, 28, 2094–2101.

Jarve, A., Todiras, M., Kny, M., Fischer, F. I., Kraemer, J. F., Wessel, N., … Bader, M. (2018). Angiotensin-(1-7) receptor Mas in hemodynamic and thermoregulatory dysfunction after high-level spinal cord injury in mice: A pilot study. *Frontiers in Physiology*, 9, 1930.

Kupfahl, C., Pink, D., Friedrich, K., Zurbrugg, H. R., Neuss, M., Warnecke, C., … Regitz-Zagrosek, V. (2000). Angiotensin II directly increases transforming growth factor β1 and osteopontin and indirectly affects collagen mRNA expression in the human heart. *Cardiovascular Research*, 46, 463–475.

Kurdi, M., & Booz, G. W. (2011). New take on the role of angiotensin II in cardiac hypertrophy and fibrosis. *Hypertension*, 57, 1034–1038.

Lujan, H. L., & Dicarlo, S. E. (2014). Increasing venous return as a strategy to prevent or reverse cardiac dysfunction following spinal cord injury. *Journal of Physiology*, 592, 1727–1728.

Mathias, C. J., Christensen, N. J., Frankel, H. L., & Peart, W. S. (1980). Renin release during head-up tilt occurs independently of sympathetic nervous activity in tetraplegic man. *Clinical Science*, 59, 251–256.

Perhonen, M. A., Franco, F., Lane, L. D., Buckey, J. C., Blomqvist, C. G., Zerwekh, J. E., … Levine, B. D. (2001). Cardiac atrophy after bed rest and spaceflight. *Journal of Applied Physiology*, 91, 645–653.

Poormasjedi-Meibod, M. S., Mansouri, M., Fossey, M., Squair, J. W., Liu, J., McNeill, J. H., & West, C. R. (2019). Experimental spinal cord injury causes left-ventricular atrophy and is associated with an upregulation of proteolytic pathways. *Journal of Neurotrauma*, 36, 950–961.

Regitz-Zagrosek, V., Fielitz, J., & Fleck, E. (1998). Myocardial angiotensin receptors in human hearts. *Basic Research in Cardiology*, 93(Suppl 2), 37–42.

Sato, T., Suzuki, T., Watanabe, H., Kadowaki, A., Fukamizu, A., Liu, P. P., … Kuba, K. (2013). Apelin is a positive regulator of ACE2 in failing hearts. *Journal of Clinical Investigation*, 123, 5203–5211.

Scherrer-Crosbie, M. (2015). Losartan: A new treatment for cardiac cachexia? *Journal of Molecular and Cellular Cardiology*, 86, 12–13.

Sharov, V. G., & Galakhin, K. A. (1984). [Myocardial changes after spinal cord injuries in humans and experimental animals]. *Arkhiv Patologii*, 46, 17–20.

Squair, J. W., DeVeau, K. M., Harman, K. A., Poormasjedi-Meibod, M. S., Hayes, B., Liu, J., … West, C. R. (2018). Spinal cord injury causes systolic dysfunction and cardiomyocyte atrophy. *Journal of Neurotrauma*, 35, 424–434.

Stevens, S. C. W., Velten, M., Youtz, D. J., Clark, Y., Jing, R., Reiser, P. J., … Wold, L. E. (2015). Losartan treatment attenuates tumor-induced myocardial dysfunction. *Journal of Molecular and Cellular Cardiology*, 85, 37–47.

Strack, A. M., Sawyer, W. B., Marubio, L. M., & Loewy, A. D. (1988). Spinal origin of sympathetic preganglionic neurons in the rat. *Brain Research*, 455, 187–191.

van Esch, J. H., Gembardt, F., Sterner-Kock, A., Heringer-Walther, S., Le, T. H., Lassner, D., … Walther, T. (2010). Cardiac phenotype and angiotensin II levels in AT1a, AT1b, and AT2 receptor single, double, and triple knockouts. *Cardiovascular Research*, 86, 401–409.

Weaver, L. C., Fleming, J. C., Mathias, C. J., & Krassioukov, A. V. (2012). Disordered cardiovascular control after spinal cord injury. *Handbook of Clinical Neurology*, 109, 213–233.

West, C. R., Crawford, M. A., Poormasjedi-Meibod, M. S., Currie, K. D., Fallavollita, A., Yuen, V., … Krassioukov, A. V. (2014). Passive hind-limb cycling improves cardiac function and reduces cardiovascular disease risk in experimental spinal cord injury. *Journal of Physiology*, 592, 1771–1783.

West, C. R., Squair, J. W., McCracken, L., Currie, K. D., Somvanshi, R., Yuen, V., … Krassioukov, A. V. (2016). Cardiac consequences of autonomic dysreflexia in spinal cord injury. *Hypertension*, 68, 1281–1289.

Williams, A. M., Gee, C. M., Voss, C., & West, C. R. (2019). Cardiac consequences of spinal cord injury: Systematic review and meta-analysis. *Heart*, 105, 217–225.

Yoshida, T., Tabony, A. M., Galvez, S., Mitch, W. E., Higashi, Y., Sukhanov, S., & Delafontaine, P. (2013). Molecular mechanisms and signaling pathways of angiotensin II-induced muscle wasting: Potential therapeutic targets for cardiac cachexia. *International Journal of Biochemistry & Cell Biology*, *45*, 2322–2332.

Zaglia, T., Milan, G., Franzoso, M., Bertaggia, E., Pianca, N., Piasentini, E., … Mongillo, M. (2013). Cardiac sympathetic neurons provide trophic signal to the heart via β2-adrenoceptor-dependent regulation of proteolysis. *Cardiovascular Research*, *97*, 240–250.